UNITED NATIONS EDUCATIONAL, SCIENTIFIC AND CULTURAL ORGANIZATION
INTERNATIONAL ATOMIC ENERGY AGENCY
INTERNATIONAL CENTRE FOR THEORETICAL PHYSICS
I.C.T.P., P.O. BOX 586, 34100 TRIESTE, ITALY, CABLE: CENTRATOM TRIESTE

H4.SMR/916 - 8

SEVENTH COLLEGE ON BIOPHYSICS:
Structure and Function of Biopolymers: Experimental and Theoretical Techniques.
4 - 29 March 1996

The Self-Assembly of Guanosine Derivatives and Folic Acid

Giovanni GOTTARELLI
Dipartimento di Chimica Organica "A Mangini"
Universita' di Bologna
Bologna
ITALY

THE SELF-ASSEMBLY OF GUANOSINE DERIVATIVES AND FOLIC ACID

GIOVANNI GOTTARELLI and GIAN PIERO SPADA
Università di Bologna, Dipartimento di Chimica Organica "A. Mangini", Via S. Donato 15, 40127 Bologna (Italy)

PAOLO MARIANI
Università di Ancona, Istituto di Scienze Fisiche Via Ranieri, 65 - 60131 Ancona (Italy)

1. Introduction

It has been known for several years that highly concentrated DNA in water forms liquid crystalline mesophases [1]. The phases have been identified as cholesteric, at lower concentration, and hexagonal, at higher concentration [2] (see Figure 1).

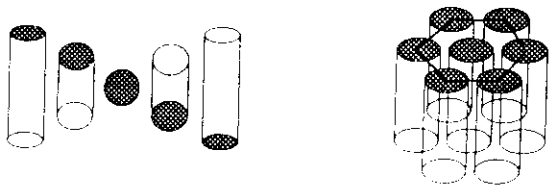

(a) *(b)*

Figure 1. Cholesteric *(a)* and hexagonal *(b)* arrangements of elongated objects, *e.g.* DNA.

Relatively short fragments of DNA (*ca.* 100 b.p.) form cholesterics which can be aligned by magnetic fields; the cholesteric axis is aligned parallel to the field (the individual double helices are instead perpendicular to the field) to give either fingerprint or planar textures (see Figure 2).

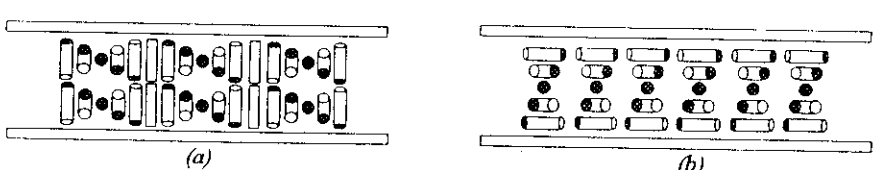

(a) *(b)*

Figure 2. Fingerprint *(a)* and planar *(b)* orientation of a cholesteric relative to the cell surface.

In the planar texture, the cholesteric helix axis is perpendicular to the cell windows; this texture is very useful for spectroscopic measurements as it shows little or no birefringence. In the fingerprint texture instead, the helix axis is parallel to the cell windows and a typical striped pattern appears; from the distance between the stripes, the cholesteric pitch can be measured [3].
The first example of mesomorphic behaviour in the guanine family concerns the dimer d(GpG) **1** [4]. Subsequently also alkaline folates **2** were reported to give liquid crystalline phases [5].

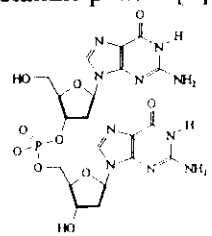

(1)

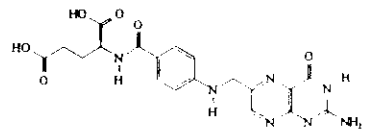

(2)

Guanine and pterine are the heterocyclic bases present in the two molecules; both bases possess a particular sequence of groups which act as donors or acceptors of hydrogen bonds. These groups are of fundamental importance in the self-recognition and self-assembly processes.

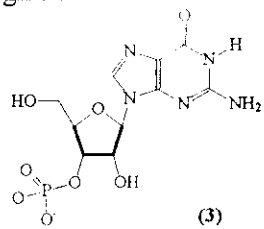

(3)

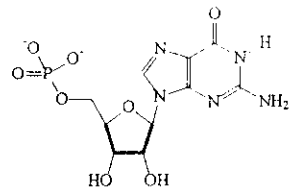

(4)

The ability of guanosine derivatives to form gels has been known for more than eighty years since the work of Bang [6]. An X-ray study of the fibre obtained from a gel of guanosine 3'-phosphate **3** allowed Gellert *et al.* [7] to propose the tetrameric arrangement depicted in Figure 3 (G-quartet) in which the four molecules are connected by a special scheme of hydrogen bonds (Hoogsteen), as a consequence of the sequence of donor and acceptor groups present in the base.

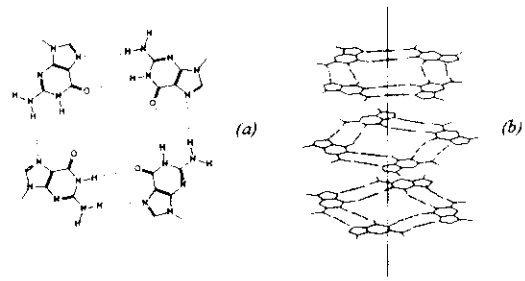

Figure 3. The tetrameric arrangement, G-quartet *(a)*, of the guanine moieties and the piling up *(b)* of three contiguous quartets.

In the aggregate, the guanosine tetramers are piled on top of one another, with sugar protruding at the periphery. However, the tetramers do not stack in

register, but are rotated with respect to each other to give an overall helical structure. In the case of guanosine 5'-phosphate **4**, a continuous helix seems instead to be formed; however, this change from the planar tetramers requires only small distortions of hydrogen bonds. If the fibre is obtained in the presence of an excess of NaCl, the planar tetramers seem to form again [8].
The same tetrameric motif was found also in the self-structure formed by polyguanylic acid by two independent fibre X-ray investigations [9,10]: the assembled species is a four-stranded, right-handed helix with parallel sugar phosphate filaments held together by the familiar G-quartets.
An extensive investigation on gels formed by several guanosine derivatives was carried out by Guschlbauer and coworkers [11]; the presence of the tetramers was assumed also in gels formed at very low concentration.
The X-ray study of the liquid crystalline phases, particularly of the more ordered hexagonal one, has given very useful information on the structure of the assembled columnar species and is of fundamental importance for the study of the self-assembly process in isotropic solution.

2. X-Ray Diffraction Structural Analysis

X-Ray diffraction analysis is a powerful and well-established technique for the determination of mesomorphic structures [12-14].
The first step in the structure analysis of a mesomorphic system is to construct the phase diagrams, *i.e.* to characterize the different phases and to determine their range of existence as a function of the usual variables, temperature and concentration. From the experimental standpoint, the techniques used for the study of lyotropic phases are those currently used in crystallography laboratories. However, the X-ray cameras must fulfill a few requirements, as the composition of the sample, especially the water content, must be kept under control and the experiments must be carried out at controlled temperature. Moreover, the X-ray diagrams must be fully explored, as the dimensions of the structure elements can be fairly large (from several hundred Å to about 10 Å) and at the same time, information on the short-range molecular organization (from about 10 Å to few Å) must be obtained. The conventional X-ray cameras generally do not satisfy all the above conditions. Most of the experiments described in this paper were therefore carried out with Guinier-type cameras of special design (see for example ref. [15]), operating *in vacuo* or in air. In all the reported experiments, the samples were held in a vacuum-tight cylindrical cell provided with thin mica windows and the sample holder was kept at constant temperature. For intensity measurements, the samples were rotated continuously during the exposure, in order to reduce spottiness arising from possible macroscopic monodomains.

The data of X-ray diffraction experiments from lyotropic samples can be analysed considering a convenient operational separation. In fact, the long-range organization of the structure elements gives rise to the reflections observed in the so-called low-angle region (scattering angle 2θ ranging from 10' to 10°), which specifies the crystalline lattice and the symmetry of the structure, while the short-range molecular organization gives rise to usually one or two reflections in the so-called high-angle region (centred around 2θ angles of about 22°) [12]. If the experiments are carried out on unoriented samples, only the spacings s (s being defined as $(2 \sin\theta)/\lambda$, where λ is the X-ray wavelength) and the intensities of the reflections are known. The problem is to index the low-angle reflections and to determine the symmetry of the lattice and the structure of the phase, discriminating the reflections that are systematically absent, because of symmetry, from those whose intensity happens to be weak for other reasons. As usual in crystallography, the symmetry of the lattice is determined by finding one equation, among those which define the spacings of the reflections for the different symmetry systems [12,16], with which all the observed spacings agree. Once the symmetry is found, the dimensions of the unit cell can be calculated. It is evident that the indexing operation must consider the possible presence of different phases coexisting in equilibrium at the same concentration: this problem is tackled by carefully exploring the phase diagram. It should be observed that the resolution of the low-angle scattering data is intrinsically low (typically in the order of 15-10 Å), as a consequence of the liquid crystalline order. Therefore, the number of observed reflections could be too small to identify the structure unambiguously. From the unit cell parameters, considering the chemical composition of the sample and on the basis of some fundamental assumptions (namely that the lyotropic molecules segregate into regions from which water is excluded and the interface between the water and the hydrophobic residues is covered by the hydrophilic groups), the shape and the dimensions of the structure elements can be obtained [12].
The final step in the structure determination is the calculation of the electron density maps and the comparison of the results with chemically independent information. In order to solve the crystallographic phase problem, several direct and indirect methods have been proposed and applied in the case of lyotropic structures [17,18]. However, some unusual constraints are encountered in these systems: due to the delicate thermodynamical phase equilibrium, the use of the isomorphous replacement technique is for example precluded. On the other hand, the modelling of the structure elements is not usually easy. In the experiments described in this paper, the phase problem has been solved by using a direct approch, based on the Shannon theorem [19]: the so-called swelling series experiment (see for example refs. [20,21]).

3. X-Ray and Neutron Small Angle Scattering Investigations of the Isotropic Phases

X-Ray (SAXS) or Neutron (SANS) Small Angle Scattering are methods for analysing the structure of colloid and macromolecular systems in solution [22-25]. A sharp and well-collimated incident beam penetrates the solution under investigation, and the radiation scattered to very small angles is measured as a function of the scattering vector Q, defined as $(4\pi \sin \theta) / \lambda$. A well-developed theory permits the derivation of several geometrical and structural parameters of the particles in solution from the scattering curve [22.23,25]. In particular, in the case of solutic s of mono-disperse particles with concentration sufficiently small for there to be no interference between waves scattered by different particles, the Guinier approximation applies: for small values of Q, the scattering intensity follows an exponential course. In logarithmic form this reads as:

$$\ln I(Q) = \ln I(Q)_{Q=0} - (R_g^2 Q^2 / 3) \quad (1)$$

Therefore, a plot of ln I(Q) versus Q^2, the so-called Guinier plot, can furnish the radius of gyration of the scattering particles (R_g, *i.e.* the square root of the mean square distance of all individual scattering centres of the particle from the centre of gravity of the particle) and the intensity scattered at zero angle, $I(Q)_{Q=0}$, which depends on the concentration and volume of the scattering particles and on the contrast (differences in electron densities or in scattering length densities between the solvent and the scattering particles in the case of X-ray and neutron scattering experiments, respectively). Likewise, in the case of rod-like particles, linear behaviour is expected in the small Q-range in a Guinier plot of the cross-section factor ln(I(Q)Q) versus Q^2, according to:

$$\ln [I(Q)\, Q] = \ln [I(Q)\, Q]_{Q=0} - (R_c^2 Q^2 / 2) \quad (2)$$

From this plot, the cross-sectional intensity scattered at Q=0 (which depends on the mass per unit length) and the radius of gyration of the cross-section R_c can be determined. A simple relationship between R_g and R_c allows the determination of the height h of the rod-like particle [25]:

$$h^2 = 12 (R_g^2 - R_c^2) \quad (3)$$

The radius of gyration R_g can be given explicitly in terms of the geometrical parameters of the scattering particles in a few simple cases [22,24].

In the series of guanosine and analogous derivatives discussed in this paper, the structural properties of the scattering particles existing in the isotropic phases were investigated both by X-ray and neutron scattering experiments [26-28]. For neutron experiments, in order to improve statistics, D_2O was used as a solvent. Guinier plots ln I(Q) versus Q^2 and ln [I(Q) Q] versus Q^2 were used to evidence the presence of cylindrical particles and to determine their dimensions. According to the structure of the cholesteric and hexagonal phases, the experimental data were fitted by using a model of rod-shaped aggregates

formed by a stacking of guanosine or folate tetramers. As a result, the number of piled tetramers could be obtained.

4. The Formation of Columnar Liquid Crystals by Deoxyguanosine Derivatives and Alkaline Folates.

2'-Deoxyguanylyl-(3'-5')-2'-deoxyguanosine **1** in water forms LC phases at relatively low concentration (2.5% w/w). Microscopic textures are indicative of the presence of a cholesteric and a hexagonal phase at lower and higher concentration respectively. The cholesteric phase can easily be aligned with a magnetic field to give a planar or a fingerprint texture without unwinding the cholesteric helix which is oriented parallel to the applied field.
This behaviour indicates that the "objects" composing the phase have negative diamagnetic anisotropy. The overall characteristics of the LC phases, including the magnetic behaviour, are very similar to those displayed by DNA with an average length of around 100 base pairs. This similarity, together with what was known about the structure of the gels and the four-stranded helix of poly(G), already give indications about a probable structure of the aggregates [4].
X-Ray experiments give evidence on the columnar nature of the different phases observed as a function of concentration and temperature. According to the diffraction profiles observed for thermotropic columnar LCs [14], a narrow band centred in the high-angle region at about $s = (3.4\ Å)^{-1}$ is indicative of a phase made of columnar structure elements; this reflection is in fact related to the nature of the intracolumnar order (see Figure 4). In our systems this is observed in both the cholesteric and hexagonal phases [29].

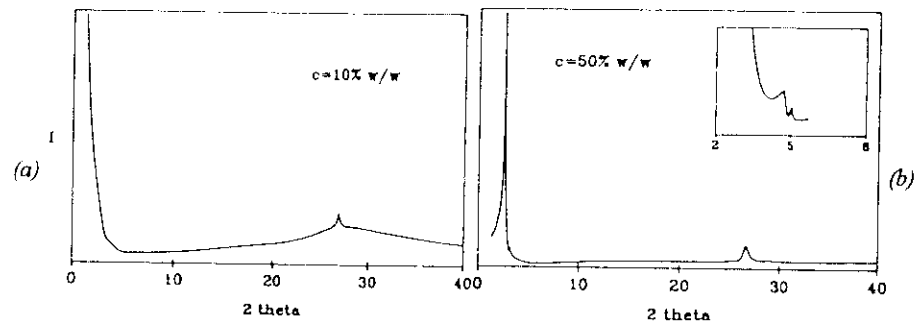

Figure 4. Typical X-ray diffraction patterns of cholesteric *(a)* and hexagonal *(b)* phases formed by **1**.

The low angle ($s < (10\ Å)^{-1}$) diffraction profile gives information on the arrangement of the columns. When the sample, observed with the optical microscope, shows the cholesteric texture, the low-angle X-ray diffraction region is characterized by only a diffuse region whose position strongly depends on the water content. This profile confirms that we are dealing with a cholesteric phase characterized by the presence of columns; the band observed refers to the mean distance between neighbouring cylinders, which changes as a function of concentration.

At higher concentrations, in correspondence to the hexagonal texture detected by optical microscopy, the low angle profiles are characterized by narrow reflections (from 3 to 5 Bragg peaks), which indicate that the phase is highly ordered (see Figure 4). The peak positions are in the order 1, $\sqrt{3}$, $\sqrt{4}$, ... and could be indexed considering a 2-D hexagonal lattice of p6m symmetry (space group No.17 of the International Tables of Crystallography [16]). For this symmetry group, the equation which defines the spacing of the reflection is in fact [12,16]

$$s_{hk} = (h^2 + k^2 - hk)^{1/2} / a \qquad (4)$$

where a is the unit cell dimension and h, k are the Miller indices of the reflections. This phase is formed by parallel columnar aggregates packed in a hexagonal array, each aggregate being surrounded by six others at a distance equal to the unit cell dimension.

At constant temperature a changes continuously as a function of the sample concentration. As is usual for chromonic phases [30] (see also ref. [12] for the corresponding behaviour of lyotropic phases), the distance between the rods increases as the water content increases. Assuming that water does not penetrate the columns and they have a circular section and infinite length, from the unit cell dimension the radius could be determined according to

$$R = (\sigma\ c_v / \pi\ N)^{1/2} \qquad (5)$$

where σ is the area of the 2-D hexagonal unit cell ($\sigma = a^2\ \sqrt{3} / 2$), N the number of columns per unit cell ($N = 1$) and c_v the d(GpG) volume concentration [31]. At room temperature, the results indicate a roughly constant radius of *ca.* 12.8 Å, in good agreement with that of the G-quartet. Similar results were obtained also for the other derivatives investigated.

From the intensity of the low-angle diffraction peaks and by "swelling" experiments, the 2-D electron density map has been determined. In particular, the phase problem has been solved considering the continuous changes of the observed intensity as a function of the water content (see ref. [20,24]). Within the same phase, one can in fact expect that at all concentrations the electron distribution of the cylinders will remain fairly constant and that the increased water content will increase only the separation between the columns. Considering that in these conditions the structure factors sample a unique continuous curve, the amplitudes of the reflections observed change continuously as a function of the s values of the reflections. From the position

of the zeros, the signs of the corresponding structure factors can be derived. In this way, an electron density map can be calculated (Figure 5).

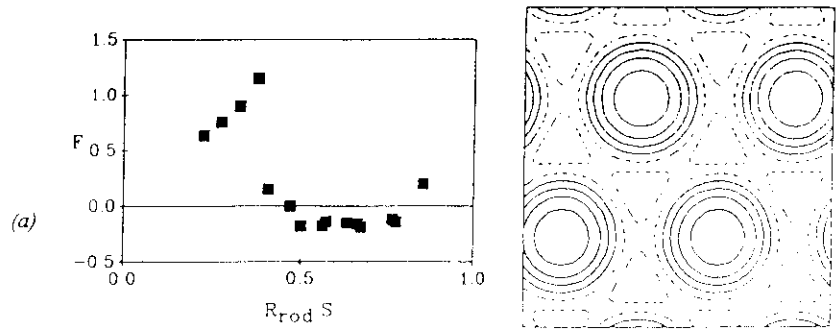

Figure 5. Determination of the signs of the structure factors *(a)* in the hexagonal phase and its electron density distribution *(b)*

The map shows clearly the electron-dense columnar projections, roughly circular; the rods appear surrounded by a smooth region of lower electron density, which is associated with water. The radius of the columnar cross-sections directly measured from the map is in very good agreement with that deduced from equation (5).

From all these data, a model for the "objects" which are the phase building blocks can be deduced: they are chiral columnar aggregates composed of a stacked array of planar or quasi-planar tetramers; the tetramers are formed by Hoogsteen-bonded guanine moieties. The tetrameric planes are stacked on top of one another, but not in register; they are rotated at a positive angle one with respect to the other to give a right-handed helix. As reported for poly(G), the sugar-phosphate backbones protrude at the periphery of the structure.

In the cholesteric phase, which exists in the low concentration part of the phase diagram, the columns are relatively free to move and their surface chirality generates the cholesteric helical structure. In the hexagonal phase, which occurs at higher concentrations, the free space available is much less and the columns are forced to adopt a more compact hexagonal packing in which the weak chiral forces are overpowered by the severe space limitations. In all cases, no long-range column-to-column correlation of the tetramer position exists as the rods may freely translate in a direction perpendicular to the two-dimensional hexagonal cell. This interpretation was confirmed by X-ray diffraction experiments on magnetically oriented samples [32].

Other guanosine derivatives which show the formation of columnar LCs, all characterized by the presence of the tetrameric motif, are compounds **5-13**. The critical concentrations for phase transitions are reported in Table 1.

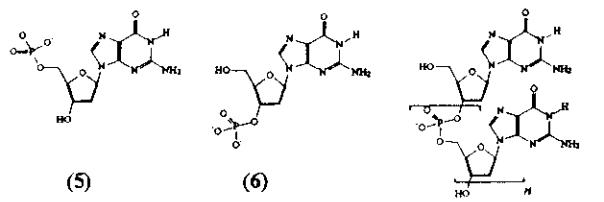

n=2 (7)

n=3 (8)

n=5 (9)

(5) (6)

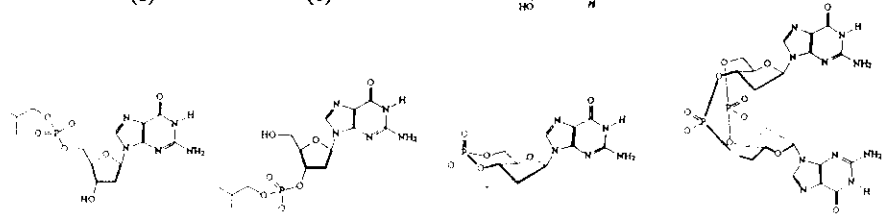

(10) (11) (12) (13)

In the homologous series d(GpG) 1, d(GpGpG) 7, d(GpGpGpG) 8 and d(GpGpGpGpGpG) 9, which possess only internucleoside phosphate groups, the critical concentration at which the cholesteric phase appears seems to follow a definite trend related to the ratio of negative charges/guanine units. This ratio is indicative of both the electrostatic repulsive interaction and the hydrophilic/hydrophobic balance, the smaller the ratio, the easier the formation of the cholesteric phase [33].

Table 1. The phase sequences and the transition concentrations for the guanosine derivatives investigated.

Compound		Counterion	Phase sequence						
(1)	d(GpG)	Na^+	I	2.5%	N*	18%			H
		K^+	I	1.5%	N*	15%			H
(7)	d(GpGpG)	Na^+	I	8%	N*	25%			H
(8)	d(GpGpGpG)	Na^+	I	13%	N*	*ca.* 35%			H
(9)	d(GpGpGpGpGpG)	Na^+	I	18-20%	N*	35%			H
(5)	d(pG)	NH_4^+	I	30%	N*	40%			H
(6)	d(Gp)	NH_4^+	I	5%	N*	35%	H_b 58% Sq	68%	H
(10)	d(*i*-Bu-pG)	NH_4^+	I						
(11)	d(Gp-*i*-Bu)	NH_4^+	I	25%	N*	38%	H_b 52% Sq	70%	H
(12)	d(cGp)	NH_4^+	I	6.5%	N*	16%			H
(13)	d(cGpGp)	NH_4^+	I			40%			H
(14)	d(GpGpApGpG)	Na^+	I	12-20%	N*	35-40%			H

Also d(GpGpApGpG) **14** forms a cholesteric and a hexagonal phase similar to the others. The critical concentrations are not very different from those of d(GpGpGpG) and d(GpGpGpGpGpG), indicating that the presence of adenine in the central position does not inhibit the self-assembly process [34].

For the other derivatives, this ratio seems of minor importance: emblematic is the example of d(pG) 5 and its mono butyl ester **10**, where the less hydrophilic molecule does not show LC phases; steric factors which affect the assembly process seem to be predominant. Also the difference in the critical concentration for the formation of the cholesteric phases of d(pG) 5 (30% w/w)

and d(Gp) **6** (5% w/w) (this molecule and its isobutyl ester **11** show also a complex polymorphism with two hexagonal and one square phase [35]) is impressive and leads to similar conclusions. On the other hand, also the gel formation [11] and the fibre structure [7,8] of the two isomers are rather different: as reported in the introduction, the former molecule seems to form a continuous helix and follows a one-step assembly process; the latter seems to follows a stepwise aggregation and gives a fibre with strictly planar tetramers [11].

It should be noticed that the cyclic monomer phosphate **12** gives both the cholesteric and hexagonal phases, therefore the columns are formed even in the absence of a free OH in the 3' or 5' position. Hydrogen bonds are therefore not essential for p. moting the vertical stacking of the tetramers. Stacking interactions and binding effects from ions seem to give dominant contributions to the formation of the columns.

Alkaline folates form, in pure water, only a hexagonal phase [5]. The overall characteristics of this phase are of the type described for the guanosine family; in particular, the diameter of the cylinders, calculated from diffraction experiments is *ca.* 30 Å and corresponds to a pterine tetramer (Figure 6).

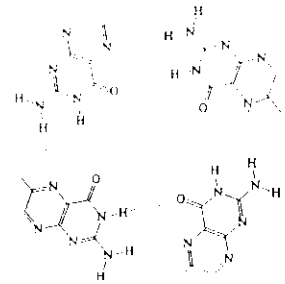

Figure 6. Tetrameric arrangement of the pterine moiety.

The critical concentration is rather high (35% w/w). However, in the presence of NaCl 1M, at *ca.* 27%, the solution becomes cholesteric. This cholesteric phase can be aligned with a magnetic fields to give planar or fingerprint textures, just like the majority of guanosine derivatives; this enables the determination of the cholesteric pitch, which is rather short (*ca.* 14 μm). All the data indicate that we are again dealing with a chiral columnar aggregate with pterine tetramers perpendicular to the long axis of the rod; the chiral glutamic residue protrudes from the column and gives the surface chirality which is related to the short pitch observed [36].

It can be noticed that for folate in pure water, a stable cholesteric phase cannot be detected; a stable cholesteric phase exists instead in the presence of an excess of Na^+ ions. Furthermore, in the case of d(GpG), the critical concentrations change in passing from the sodium (I 2.5% N* 18% H) to the potassium salt (I 1.5% N* 15% H). Also for d(pG), the critical concentration diminishes remarkably in passing from pure water to a 4M KCl solution [37].

In order to explain these and other experimental data, one has to understand the process of growth of the columns and their stability as a function of the concentration and ions present both in isotropic solution and in the mesomorphic state.

5. The Self-Assembly Process in Isotropic Water Solution

Small Angle Neutron Scattering (SANS) is a powerful technique for studying the shape and dimentions of assembled species in isotropic solution.
SANS experiments were carried out in pure D_2O for d(pG), d(GpG), d(GpGpG), d(GpGpGpG) and d(GpGpGpGpGpG) at 1 and 1.5% w/w concentrations [26]; except for d(pG), all the compounds revealed the presence of aggregates with a cylindrical shape. Modelling the cylinders with the radius of the guanosine tetramer, as deduced from X-ray work on the hexagonal phases, their length can be extracted. Furthermore, from the analysis of the scattered intensity at zero angle, one can also deduce the number of scattering particles per unit volume and hence the percent of aggregation. The results [26] are reported in Table 2.

Table 2. The number (N) of scattering particles per unit volume (10^{-17} cm^3), the percent aggregation and the length (L) of the columnar aggregates formed by homoguanylic derivatives at 1 and 1.5% w/w concentration as deduced from SANS experiments.

		(1) d(GpG)	(7) d(GpGpG)	(8) d(GpGpGpG)	(9) d(GpGpGpGpGpG)
c=1%	L (Å)±3.0	69.2	62.1	62.9	59.7
	Aggregation (%)	43.6	36.6	33.1	35.8
	N	1.10	1.00	0.89	0.99
c=1.5%	L (Å)±3.0	71.2	69.1		
	Aggregation (%)	50.2	39.0		
	N	1.84	1.43		

The length of the aggregates decreases very slowly in passing from the dimer to the hexamer and the same seems to happen also for the aggregation percent. At 1.5% concentration, the aggregation increases *ca.* 10%. All the data reported refer to freshly prepared solutions not treated thermically. In certain cases, the thermal history of the sample plays an important role in determining the dimensions of the aggregates.
The effect of thermal cycles and ions has been studied in some detail by a strictly related technique, Small Angle X-ray Scattering (SAXS) [27]; the geometrical parameters obtained by measurements carried out on 1% solutions in water with and without added electrolytes are reported in Table 3.

The different behaviour of the Na and K salts of d(GpG) is remarkable: at 20°C, both salts show observable cylinders with comparable length; at 60°C (above the melting temperature as determined by CD), in both cases no aggregates could be detected; after cooling again to 20°C, only the K salt again shows cylindrical aggregates, which are, incidentally, slightly longer than for the freshly prepared sample, while the Na salt does not show detectable aggregates.
The effect of an added excess of ions is also remarkable: in the presence of an excess of NaCl or KCl, at 60°C no melting is observed and, after cooling, slightly longer aggregates are formed.

Table 3. The length of the columnar aggregates formed by d(GpG) **1** at 1% w/w concentration as deduced from SAXS experiments (n.d.: not detectable)

		T	L(Å)
In water	Na salt	20°C	70±15
		60°C	n.d.
		20°C after cooling	n.d.
	K salt	20°C	76.7±6.9
		60°C	n.d.
		20°C after cooling	94±11
In KCl 1 M	Na salt	20°C	96.4±7.2
		60°C	95±10
		20°C after cooling	107±10
	K salt	20°C	110.8±8.8
		60°C	111.5±4.7
		20°C after cooling	119.1±6.4

The self-assembly process of all these chiral molecules can easily and conveniently be followed by CD spectroscopy. The spectra of the isolated monomeric species can be observed in diluted solutions without added salts or, in more concentrated solutions at higher temperature; they are usually drastically different from those of the assembled species. For assembled species, exciton double signed bands are often observed in correspondence to a single absorption band [38]; the spectra become similar to those of biological polymers (DNA, proteins). The technique is very useful also for measuring melting temperatures and can be more sensitive and selective than ordinary absorption measurements.
In the case of guanosine derivatives, several advantages are available in interpreting CD spectra: first, the CD spectra of the four-stranded helices of poly(G) and poly(dG) are known and also the structure of this unusual helix, which is similar to our columnar aggregates, is known in detail from fibre X-ray work on poly(G): the helix is right-handed and the G-quartets are stacked

perpendicularly to the helix axis [9,10]. Secondly, the spectroscopic properties of guanine have been extensively investigated. Consequently, it is possible to calculate the CD spectra of poly(G) and similar molecules with a relatively simple exciton treatment [39,40], having a reliable model with which to check the calculations.

From this approach, the chirality of the columnar aggregates could be deduced: in the low-energy part of the spectrum, the guanine chromophore displays two well-characterized electronic transitions corresponding to an absorption maximum at *ca.* 250 nm and to a shoulder at *ca.* 280 nm. In the four-stranded helix of poly(G), the transition at *ca.* 250 nm gives rise to a non-symmetric exciton couplet with a stronger positive component at *ca.* 260 nm and a weaker negative band at ca. 240 nm. The second transition appears as a shoulder of the positive 260 nm band.

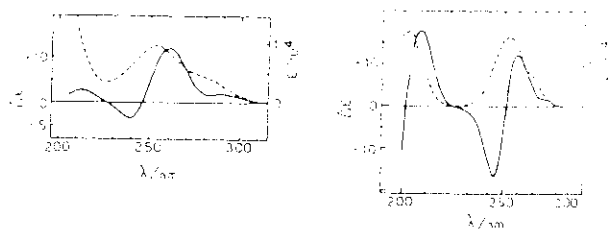

Figure 7. The experimental (left) and simulated (right) absorption (dashed line) and CD (full line) spectra of poly(G)

It follows that, whenever the columnar deoxyguanosine aggregates give similar spectra, it is possible to assign a right-handed absolute stereochemistry. The correlation has both empirical and theoretical validity.

From the sign of the CD couplet centred at *ca.* 250 nm, the absolute handedness reported in Table 4 can be deduced.

Table 4. The columnar helicity (as deduced by the exciton CD corresponding to the guanine chromophore; - and + signs refer to left and right handedness, respectively) and the cholesteric helicity and pitch for guanosine and pterine derivatives.

Compound		Columnar helicity	p (μm)	Cholesteric helicity
d(Gp)	(**6**)	(-)		*M*
d(Gp-*i*-Bu)	(**11**)	(-)		*M*
d(pG)	(**5**)	(-)	-31	*M*
d(GpG)	(**1**)	(+)	-70	*M*
d(GpGpG)	(**7**)	(+)	+140	*P*
d(GpGpGpG)	(**8**)	(+)	+100	*P*
d(GpGpGpGpGpG)	(**9**)	(+)	+43	*P*
Sodium Folate + NaCl	(**2**)		-14	*M*

Other information on the geometry of the columns can be deduced. In derivatives d(pG), d(GpGpG), d(GpGpGpG), d(GpGpGpGpGpG) [33] and

d(cGp), the band shapes are similar to poly(G) , the CD spectrum is dominated by the 260 nm band which is positive for d(GpGpG), d(GpGpGpG) and d(GpGpGpGpGpG), and negative for d(pG) and d(cGp). However, d(GpG) displays a positive 260 nm band in the presence of K^+ or Sr^{2+} ions or a positive 290 nm band in the presence of Rb^+ or Cs^+; with Na^+, both 260 and 290 nm bands are observed. The 260 or 290 nm bands have been discussed also for the assembled species of G-rich oligonucleotides connected to telomere repeat sequences [41].

From the stereochemical point of view, the presence of the 260 nm band seems to be associated to a rather regular structure, similar to that of poly(G), with the tetrameric planes perpendicular to the helix axis, while a dominant 290 nm band indicates consistent variations with respect to this situation [27,39,40].

The finding that K^+ ions allow the passage from a distorted to a regular structure is related to the size of this ion, which is ideal for positioning itself between two adjacent tetrameric planes, coordinating all eight sorrounding oxygen atoms [8].

For d(GpG), indication of the stability of the aggregates in terms of melting temperatures (T_m) were obtained by a detailed variable temperature CD investigation [27]. The stabilizing effect of the different ions, as deduced from melting temperatures, are in the order: $Sr \approx K > Rb > Na > Cs$.

The results are in excellent agreement with those from SAXS reported above: the conditions which favour a lengthening of the columns are the same as those which increase T_ms; in particular, the effect of K^+ ions is remarkable. We have therefore parallel behaviour of stability and length of the aggregates, both factors playing an important role in the LC formation.

In the case of folates, in pure D_2O no scattering aggregates can be detected by SANS even at a relatively high concentration (4% w/w) [28]. At the same concentration and with an excess of Na^+ or K^+ ions instead, the presence of scattering aggregates can be detected. The aggregates are cylindrical and, assuming a diameter of *ca.* 30 Å, as deduced from X-ray work on the hexagonal phase [5,36], the length of the cylinders can be calculated: the aggregates are composed of a stack of *ca.* 9 disks [28].

As data on the pterine electronic transitions are not reported in the literature, CD spectroscopy can be used only empirically. In particular, no information on the handedness of the columnar aggregates can be deduced. CD spectra indicate very clearly the presence of aggregates also at lower concentrations (beginning at 10^{-4} M), for which no SANS signals can be measured; this points to the formation of aggregates of smaller dimensions, too small to be detected by the scattering technique. As will be reported in the next section, the folate column length varies considerably with the concentration.

For the assembled folates, rather different spectra are obtained in pure water and in the presence of an excess of Na^+ and K^+ ions. The spectra in pure water

display single melting to give the spectrum of the free folate. The spectra obtained in the presence of salts give a clear double melting.
These results, together with NOESY and NOE data, were interpreted considering the existence of two assembled forms: one (with added ions) is more compact, and has a stronger tetramer-to-tetramer interaction; the other has a different stereochemistry of the aromatic core region and a weaker tetramer-to-tetramer interaction. In both cases, the glutamic chains are rather mobile [28].
These data in isotropic solutions are in full agreement with those obtained in the mesomorphic state and reported in the next section.
In the case of folates, as for guanine derivatives, the polymorphism observed is related to the growth of the columnar aggregates; the factors which promote the growing process lower the transition concentrations and stabilize in particular the cholesteric phases.

6. Column Length and Growth in the Mesomorphic State

The structural properties of the columns can be derived from the variation of the hexagonal cell dimension a, and (tentatively) of the main distance between the cylinders in the cholesteric phase, as a function of the volume concentration c_v. Further information can be obtained by the analysis of shape and position of the high angle 3.3 Å peak.
Assuming that in the hexagonal phase the columns are infinitely long and have a circular section with radius R, the relation between the cross-section area of the rod and the two-dimensional hexagonal unit cell surface is [12]

$$\pi R^2 = (\sqrt{3} / 2)\, a^2\, c_v \qquad (6)$$

In the columnar system discussed, the structure of the disk-shaped G-quartets is not expected to change as a function of concentration [42,43], so R can be considered constant. For infinite cylinders therefore, a will change with the volume concentration as

$$a = (2 \pi R^2 / \sqrt{3})^{1/2}\, c_v^{-1/2} \qquad (7)$$

This means that the rods move apart only laterally as dilution proceeds.
If the rod length is finite, the cylinders pack in the two-dimensional hexagonal cell again with parameter a, but also with an average vertical distance C between the cylinder centres. If L is the length of the cylinders, one obtains

$$L \pi R^2 = C (\sqrt{3} / 2)\, a^2\, c_v \qquad (8)$$

therefore the variation of a with c_v depends on the variation of the ratio L/C, *i.e.* the fraction of water in the C direction. In particular, the relationship $a \propto c_v^{-1/3}$ can be demonstrated when the interparticle distances decrease uniformly in the three dimensions as a function of concentration (*i.e.* when $L/C = 2R/a$ in the hexagonal domain) [36,37,43,44].

The two situations can be interpreted in terms of length and flexibility [45,46,47] of the aggregates: a $c_v^{-1/2}$ dependence may be indicative of infinite (with respect to the lateral distance) cylinders, while a $c_v^{-1/3}$ dependence may be interpreted in terms of finite cylinders.

The columnar stacking of the teramers can be studied in more detail by the analysis of the high-angle ($s = (3.4\ Å)^{-1}$) peak. By fitting a gaussian and a locally linear background to every peak, one can have an accurate value of the position of the peak, from which the distance between the stacked G-quartets is obtained, and of its width at half maximum, which is correlated to the average number of stacked tetramers in one column.

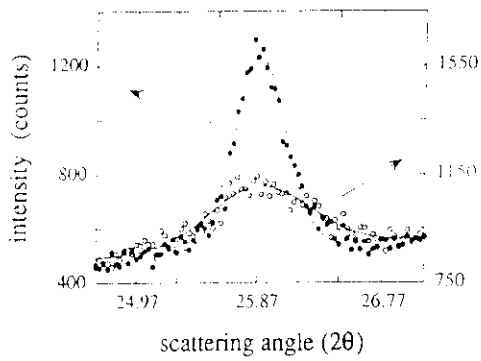

Figure 8. High angle diffraction peak ($s = (3.4Å)^{-1}$) observed at c = 50% (closed circles) and 23% (open circles) for d(pG) in KCl 4 M.

To obtain this value, numerical simulations of the scattering profile of the columnar aggregates must be performed: the tetramers were approximated by homogeneous disks with a thickness of 2.35 Å [36,37].The scattering amplitude of n of these disks, stacked one above the other at a distance of 3.4 Å, was summed up, squared and averaged over all orientations. This procedure is correct as long as there is no 3-dimensional correlation between the positions of the tetramers in different columnar aggregates. The average number of stacked discs in one column was determined by comparing the calculated and measured peak width; the average correlation length was obtained by multiplying n by the experimental stacking distance. Using these approaches and considering the results for the self-assembly in the isotropic solutions (preceding section), the pictures reported in Figure 9 can be obtained.

In the case of d(GpG), the dependence is of the -1/3 type in the cholesteric phase and indicates finite cylinders, while in the hexagonal phase infinite cylinders seem to be present. The cross-over between finite and infinite objects is near the N* to H transition [32]. The description which can be deduced is that the aggregate length grows rather quickly with concentration in the

isotropic and in the cholesteric phase. In the hexagonal phase, they are so long that their length cannot be compared to the lateral distance.

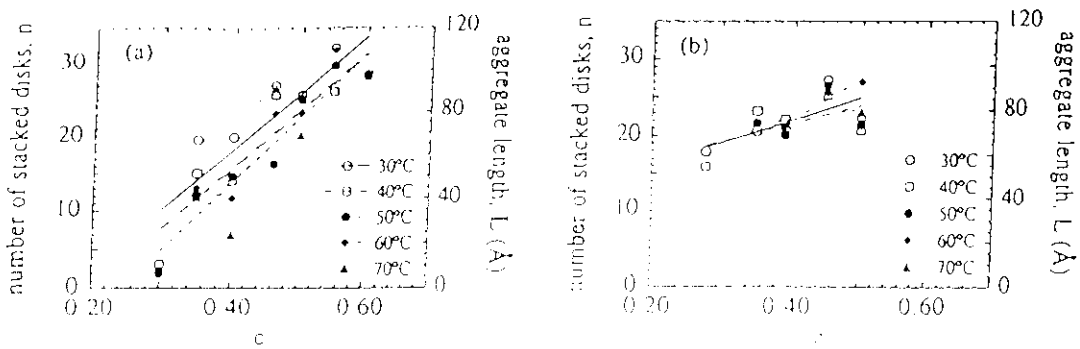

Figure 9. Number of stacked disks (and the aggregate length) as a function of folate concentration (w/w) for different temperature for disodium folate in water (a) and in NaCl 1 M (b)

In the case of derivative d(pG) instead, the columns seem to be finite also in the hexagonal phase and the length growth seems to be slow [37]. The fact that SANS is unable to detect aggregates at 1% concentration is in agreement with this result. For stereochemical and, to a lesser extent also for hydrophilicity reasons, the assembly process of d(pG) seems to be difficult. Accordingly, the critical concentration at which the N* phase appears is much higher than for d(GpG).

Also for folates with and without added salts, the -1/3 exponent indicates the formation of finite cylinders in the hexagonal phase [36]. In pure water, the distance between the disks increases as a function of the water content and temperature. The average length of the aggregates increases continuously, as a function of concentration, from 5 piled disks at the I to H transition to *ca.* 30 at a 60% concentration. In NaCl instead, the stacking distance remains almost constant, as does the size of the aggregates: also at low concentration one has *ca.* 20 piled disks.

The stabilisation operated by Na^+ ions (and, to a lesser extent, by K^+), seems similar to that described above for K^+ in the guanine system.

This behaviour is in full agreement with the results obtained by SANS in isotropic solution: at 4% concentration, no aggregates could be detected in pure water, while, in NaCl, the data indicate the presence of aggregates composed of *ca.* 9 disks [28].

The formation of a stable cholesteric mesophase only in the presence of NaCl is related to the fact that only in this condition are the aggregates long enough at relatively low concentration (*ca.* 27% w/w). Without added salts one needs a

higher concentration to obtain aggregates long enough to give a mesophase, and, at these concentrations, there is no space available for the formation of the cholesteric helix; the more compact H phase is therefore observed.
This picture is in good agreement with the theoretical prediction of phase diagrams for assembling lyotropics obtained recently by Taylor and Herzfeld [45].The calculated phase diagrams display a nematic between the isotropic and the hexagonal phases only when the aggregation is strong; for weak aggregation the direct I to H transition is predicted.

7. Stereochemistry of the Chiral Packing in the Cholesteric Mesophases

Data on the handedness and pitch of the cholesteric columnar mesophases can be obtained by using the magnetic alignment described above.The determination of the pitch values is carried out by measuring the spacing between the lines of the fingerprint textures. The determination of the cholesteric handedness is carried out by CD spectroscopy on samples with planar alignment (in order to avoid artefacts connected to strong birefringence of the sample) [48]. As reported in ref. [48] a positive CD in the absorption region indicates a right-handed cholesteric, a negative CD a left-handed cholesteric. The handedness was confirmed by recording the CD spectra in the presence of ethidium bromide which intercalates into four-stranded oligoguanylates [33]. The handedness and pitch values are reported in Table 4.
With the exception of d(GpG), in all the deoxyguanosine oligomers investigated, right-handed columns generate right-handed cholesterics.
A model for the packing of hard helical screws, which recognize their reciprocal chirality and spontaneously generate an overall helical structure, is reported in Figure 10.

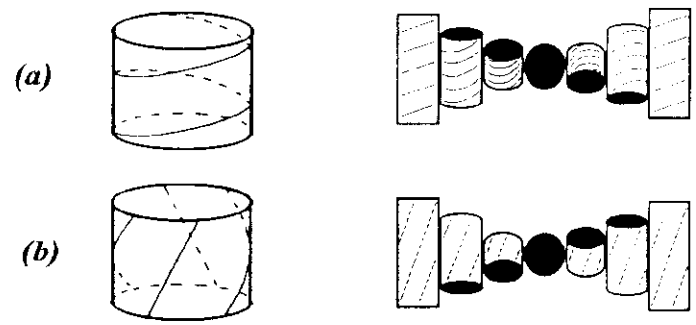

Figure 10. The different handedness of the packing of right-handed helices with different pitch-to-diameter ratios.

The model gives a simplified picture of the interaction, by hard-core repulsion only, of chiral columns in the cholesteric phase. In the model of Figure 10,

right-handed screws pack to give a right-handed superstructure. However, the model is sensitive not only to the handedness of the screws, but also to the ratio pitch/diameter of the individual objects: for a given handedness of the screws (*e.g.* right-handed) one can obtain a definite handedness of the superstructure (*e.g.* right-handed) only if $p/d < \pi$; if $p/d > \pi$ an opposite-handed superstructure is generated [48].

It is certainly an oversimplification to compare the cholesteric phases given by the guanine derivatives to the model of Figure 10 in which neither charges nor dispersive interactions nor excluded volume effects exist. Furthermore, the geometry of the four-stranded aggregates is complex and it is impossible to evaluate precisely the external diameter of the cylinders. Nevertheless, this model, which has a critical value of the p/d ratio of the individual screws around which there is an inversion of the superhelical handedness, has some utility: it gives a qualitative indication of the effect that a process of winding or unwinding the helical aggregates might have on the cholesteric handedness.

If we consider the guanine columnar assembled species as screws (the fact that they are four-stranded helices does not affect qualitatively the results), all the screws but that derived from d(GpG) behave as if their p/d ratio is smaller than the critical value. For d(GpG) the helical system seems to be unwound to give p/d larger than the critical value.

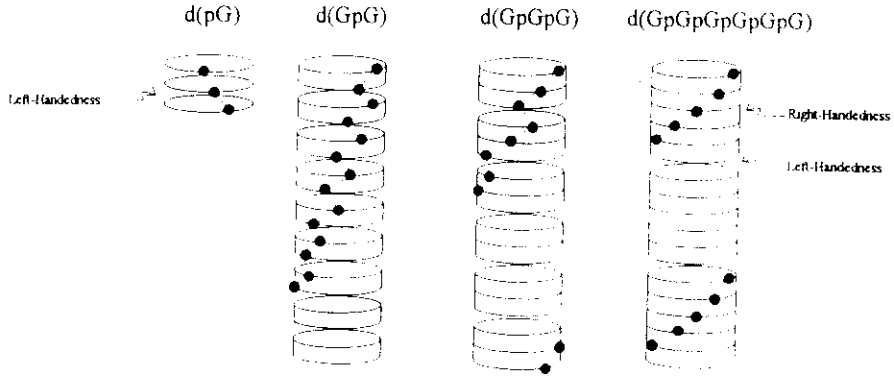

Figure 11. A representation of the chiral columnar aggregates formed by oligoguanylate derivatives (the filled circles represent the sugar units; for clarity, only one sugar per tetramer is shown).

In the homologous series d(GpG), d(GpGpG), d(GpGpGpG) and d(GpGpGpGpGpG), in which only internucleoside phosphate groups are present, the different characteristics of the cholesterics and also the opposite sign displayed by d(GpG) can be understood: in order to construct an aggregate composed of 18 disks (which for example is the average length observed by SANS in isotropic solutions of *ca.* 1% concentration), in the case of d(GpGpGpGpGpG), three discrete tetrameric aggregates have to be connected by two sets of similar non-covalent interactions (stacking forces and probably

also hydrogen bonds between the free 3' and 5' OH groups) (Figure 11). In the case of d(GpG) instead, nine discrete aggregates have to be connected by seven sets of non-covalent interactions.

It is known from X-ray work and CD data on poly(G) and poly(dG) that the four-stranded structures are right-handed, and the same applies also to the aggregates formed by homoguanylic oligomers (even if in the case of d(GpG), in the absence of added K^+, the CD intensity is much weaker). The phosphodiester linkages between the tetrameric planes is therefore connected to a right-handed structure. The contribution of non-covalent interactions to the helical handedness is not necessarily of the same sign. Let us assume that they are of the opposite sign, or maybe of the same sign but with a smaller angle of rotation between the G-quartets; in both cases, they cause unwinding of the four-stranded helices.

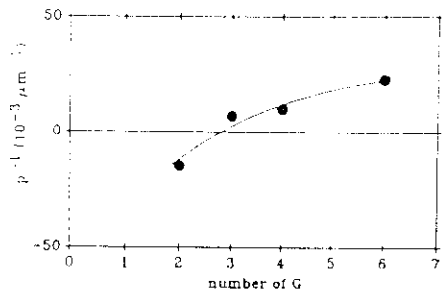

Figure 12. Reciprocal pitch of the cholesterics obtained from oligoguanylates (+ and - refer to left and right-handed cholesterics, respectively)

The unwinding effect is obviously greater for d(GpG) > d(GpGpG) > d(GpGpGpG) > d(GpGpGpGpGpG). In the case of d(GpG), it is not surprising that we have an inversion of the sense of packing as a result of the increased p/d ratio, which could be greater than the critical value.

The variation of the reciprocal pitch of the cholesterics with the number of guanosine residues is in full agrement with this hypothesis: the value p^{-1} (which is a measure of the twist between the chiral columns in the cholesteric phase) varies smoothly with the number of residues as predicted from the screw model. The assumption that the columns are formed by packing of discrete objects, for which we have some evidence from CD spectra for d(GpG) and higher oligomers (in the case of d(GpG), also a continuous aggregation mechanism could be operative in some cases), is not a necessary prerequisite and a similar reasoning could apply also to a continuous assembly model.

With regard to this point, the high-resolution crystal structure of the hexanucleotide d(TpGpGpGpGpT) in the presence of Na^+ ions, reported very recently [49], is particularly instructive. The usual G-quartets are present and connect four molecules of the oligonucleotide with parallel strands. In the

crystal, two of these aggregates are connected coaxially by a sodium ion in a head-to-head way to give a cylindrical structure formed by G-quartets. The terminal thymine molecules protrude from the cylindrical, structure which is similar to a right-handed four-stranded helix.

Acknowledgement

We thank Consiglio Nazionale delle Ricerche (Italy) and Ministero dell'Università e della Ricerca Scientifica e Tecnologica (Italy) for financial support.

References

1. Robinson, C. (1961) Liquid crystalline structure in polypeptide solutions, *Tetrahedron* **13**, 219-234.
2. Livolant, F., Levelut, A. M., Doucet, J., and Benoit, J. P. (1989) The highly concentrated liquid-crystalline phase of DNA is columnar hexagonal, *Nature* 339, 724-726, and references therein.
3. Spada, G. P., Brigidi, P., and Gottarelli, G. (1988) The determination of the handedness of cholesteric superhelices formed by DNA fragments, *J. Chem. Soc., Chem. Commun.*, 953-954.
4. Spada, G. P., Carcuro, A., Colonna, F. P., Garbesi, A., and Gottarelli, G. (1988) Lyomesophases formed by the dinucleoside phosphate d(GpG), *Liq. Cryst.* **3**, 651-654.
5. Bonazzi, S., De Morais, M. M., Gottarelli, G., Mariani, P., and Spada, G. P. (1993) Self-assembly and liquid crystal formation of folic acid salts, *Angew. Chem., Int. Ed. Engl.* **32**, 248-250.
6. Bang, I. (1910) Guanylic acid, *Biochem. Z.* **26**, 293-311.
7. Gellert, M., Lipsett, M. N., and Davies, D. R. (1962) Helix formation by guanylic acid, *Proc. Natl. Acad. Sci. USA* **48**, 2013-2018.
8. Saenger, W. (1984) *Principles of Nucleic Acid Structures*, Springer, New York, pp. 315-320; and references therein.
9. Arnott, S., Chandrasekaran, R., and Martilla, C. M. (1974) Structures for polyinosinic acid and polyguanylic acid, *Biochem. J.* **141**, 537-543.
10. Zimmermann, S. B., Cohen, G. H., and Davies, D. R. (1975) X-ray fiber diffraction and model building study of polyguanylic acid and polyinosinic acid, *J. Mol. Biol.* **92**, 181-192.
11. Guschlbauer, W., Chantot, J. F., and Thiele, D. (1990) Four-stranded nucleic acid structures 25 years later: from guanosine gels to telomer DNA, *J. Biomolec. Struct. & Dynam.* **8**, 491-511; and references therein.
12. Luzzati, V. (1968) X-ray diffraction studies of lipid-water systems, in D. Chapman (ed.) *Biological Membranes*, Academic Press, London, pp. 71-123.
13. Mariani, P., Rustichelli, F., and Torquati, G. (1991) Structure of mesophases: X-ray diffraction, in R. Bartolino, L. Fronzoni and F. Simoni (eds.), *Physics of Liquid Crystals*, Gordon and Breach, New York, pp. 3-44.

14. Weber, P., Guillon, D., and Skoulios, A. (1991) Hexagonal columnar mesophases from phtalocyanine. Upright and tilted intracolumnar molecular stacking, herringbone and rotationally distorted columnar packing, *Liq. Cryst.* **9**, 369-382.
15. Tardieu, A. (1972) Etude Cristallographique de systemes lipides-eau, Ph. D. Thesis, Université Paris Sud.
16. (1952) International Tables for X-ray Crystallography, The Kynoch Press, Birmingham.
17. Luzzati, V., Gulik-Krzywicki, T., and Tardieu, A. (1968) Polymorphism of lecithins, *Nature* **218**, 1031-1034.
18. Luzzati, V., Mariani, P., and Delacroix, H. (1991) X-ray crystallography at macromolecular resolution: a solution of the phase problem, *Makromol. Chem. Macromol. Symp.* **15**, 1-17.
19. Sayre, D. (1952) Some implications of a theorem due to Shannon, *Acta Cryst.* **5**, 843-843
20. Franks, N. P. (1976) Structural analysis of hydrated egg lecithin and cholesterol bilayers. I. X-ray diffraction, *J. Mol. Biol.* **100**, 345-358.
21. Gulik, A., Luzzati, V., De Rosa, M., and Gambacorta, A. (1985) Structure and polymorphism of bipolar isopranyl ether lipids from Archaebacteria. *J. Mol. Biol.* **182**, 131-149.
22. Guinier A. and Fournet, G. (1955) *Small angle scattering of X-rays*, Wiley, New York.
23. Jacrot, B. (1976) The study of biological structures by neutron scattering from solution, *Rep. Prog. Phys.* **39**, 911-953.
24. Chen, S. H. and Lin, T. L. (1987) Colloidal solution, in R. Celotta and J. Levine (eds.) *Methods in Experimental Physics*, Vol.23; D. L. Price and K. Skold (eds.), *Neutron Scattering*, Part B, Academic Press, New York, pp. 489-543.
25. (1982) Glatter, O. and Kratky, O. (eds.) *Small Angle X-ray scattering*, Academic Press, New York.
26. Carughi, F., Ceretti, M., and Mariani, P. (1992) Structural organization of guanosine derivatives in dilute solutions: small angle neutron scattering analysis, *Eur. Biophys. J.* **21**, 155-161.
27. Bonazzi, S., Gottarelli, G., Spada, G. P., Mariani, P., Romanzetti, S., Garbesi, A., and La Monaca, A. (1995) A study of the self-assembly of 2'-deoxyguanylyl-(3'-5')-2'-deoxyguanosine, d(GpG), by SAXS and CD, *Gazz. Chim. (It.)*, in press.
28. Carsughi, F., Di Nicola, G., Gottarelli, G., Mariani, P., Mezzina, E., Sabatucci, A., and Spada, G. P. (1995) The self-recognition and self-assembly of folic acid salts in isotropic water solution, *J. Am. Chem. Soc.*, submitted.
29. Mariani, P., Mazabard, C., Garbesi, A., and Spada, G. P. (1989) A study of the structure of the lyomesophases formed by the dinucleoside phosphate d(GpG). An approach by X-ray diffraction and optical microscopy, *J. Am. Chem. Soc.* **111**, 6369-6373.
30. Perahia, D., Luz, Z., Wachtel, E. J., and Zimmermann, H. (1987) NMR and X-ray diffraction of the 7,7'-disodiumchromoglycate-water lyomesophases, *Liq. Cryst.* **2**, 473-489.
31. Iball, J., Morgan, C. H., and Wilson, H. R. (1963) Fibres of guanine nucleosides and nucleotides, *Nature* **150**, 688-689.

32. Amaral, L. Q., Itri, R., Mariani, P. and Micheletto, R. (1992) Structural study of the aggregates formed by the dinucleoside phosphate G2 in aqueous solution, *Liq. Cryst.* **12**, 913-919.
33. Bonazzi, S., Capobianco, M., De Morais, M. M., Garbesi, A., Gottarelli, G., Mariani, P., Ponzi Bossi, M. G., Spada, G. P., and Tondelli, L. (1991) Four-stranded aggregates of oligodeoxyguanylates forming lyotropic liquid crystals: a study by circular dichroism, optical microscopy, and X-ray diffraction, *J. Am. Chem. Soc.* **113**, 5809-5816.
34. Bonazzi, S., Garbesi, A., Gottarelli, G., Spada, G. P., and Mariani, P.; manuscript in preparation.
35. Mariani, P., De Morais, M. M., Gottarelli, G., Spada, G. P., Delacroix, H., and Tondelli, L. (1993) Structural analysis of the lyotropic polymorphism of four-stranded aggregates of 2'-deoxyguanosine 3'-monophosphate derivatives, *Liq. Cryst.* **15**, 757-778
36. Ciuchi, F., Di Nicola, G., Franz, H., Gottarelli, G., Mariani, P., Ponzi Bossi, M. G., Spada, G. P. (1994) Self-recognition and self-assembly of folic acid salts: columnar liquid crystalline polymorphism and the column growth process, *J. Am. Chem. Soc.* **116**, 7064-7071.
37. Franz, H., Ciuchi, F., Di Nicola, G., De Morais, M. M., and Mariani, P. (1994) Unusual lyotropic polymorphism of deoxyguanosine-5'-monophosphate: X-ray diffraction analysis of the correlation between self-assembling and phase behaviour, *Phys. Rev. E* **50**, 395-402.
38. Mason, S.F. (1982) *Molecular Optical Activity and the Chiral Discrimination*, Cambridge University Press, Cambridge.
39. Cech, C.L. and Tinoco,I., Jr. (1976) Circular dichroism calculations for polyinosinic acid in proposed multi-strand geometries, *Nucl. Acid Res.* **3**, 399-404.
40. Gottarelli, G., Palmieri, P., and Spada, G. P. (1990) On the exciton optical activity of the four-stranded helix of poly(G), *Gazz. Chim. (It.)* **120**, 101-107.
41. Balagurumoorthy, P., Brahmachary, S. K., Mohanty, D., Bansal, M., and Sasisekharan, V. (1992) Hairpin and parallel quartet structures for telomeric sequences, *Nucl. Acid Res.* **29**, 4061-4067.
42. Zimmerman, S.B. (1976) X-ray study by fiber diffraction methods of a self-aggregate of guanosine-5'-phosphate with the same helical parameters as poly(rG), *J. Mol. Biol.* **106**, 663-672.
43. Amaral, L. Q., Gulik, A., Itri, R., and Mariani, P. (1992) Micellar hexagonal phases in lyotropic liquid crystals, *Phys. Rev. A* **46**, 3548-3550.
44. Mariani, P. and Amaral, L. Q. (1994) Micellar growth in hexagonal phases of lipid systems, *Phys. Rev. E* **50**, 1678-1681.
45. Taylor, M.P. and Herzfeld, J. (1991) Shape anisotropy and orderd phases in reversibly assembling lyotropic systems, *Phys. Rev. A* **43**, 1892-1905.
46. Hentschke, R. and Herzfeld, J. (1991) Isotropic, nematic, and columnar ordering in systems of persistent flexible hard rods, *Phys. Rev. A* **44**, 1148-1155.
47. Hentschke, R. (1991) Effect of persistent flexibility on the isotropic, nematic and columnar ordering in self-assembling systems, *Liq. Cryst.* **10**, 691-702.

48. Gottarelli, G., Spada, G. P. (1994) Application of CD to the study of some cholesteric mesophases, in K. Nakanishi, N. Berova, and R. W. Woody (eds.), *Circular Dichroism, Principles and Applications*", VCH, New York, pp. 105-119.
49. Laughlan, G., Murchie, A. I. H., Norman, D. G., Moore, M. H., Moody, P. E. C., Lilley, D. M., Luisi, B. (1994) The high-resolution crystal structure of a parallel-stranded guanine tetraplex, *Science* **265**, 520-524.